

NASA Technical Memorandum 107062  
AIAA-95-2822

11-20  
6273  
p- 17

## Performance of a Miniaturized Arcjet

(NASA-TM-107062) PERFORMANCE OF A  
MINIATURIZED ARCJET (NASA, Lewis  
Research Center) 17 p

N96-15326

Unclass

G3/20 0081582

John M. Sankovic  
*Lewis Research Center*  
*Cleveland, Ohio*

and

David T. Jacobson  
*The Ohio State University*  
*Columbus, Ohio*

Prepared for the  
31st Joint Propulsion Conference and Exhibit  
cosponsored by AIAA, ASME, SAE, and ASEE  
San Diego, California, July 10-12, 1995



National Aeronautics and  
Space Administration

# PERFORMANCE OF A MINIATURIZED ARCJET

John M. Sankovic\*  
National Aeronautics and Space Administration  
Lewis Research Center  
Cleveland, Ohio

and

David T. Jacobson\*\*  
The Ohio State University  
Columbus, Ohio

## ABSTRACT

Performance measurements were obtained and life-limiting mechanisms were identified on a laboratory-model arcjet thruster designed to operate at a nominal power level of 300 W. The design employed a supersonic-arc-attachment concept and was operated from 200 to 400 W on hydrogen/nitrogen mixtures in ratios simulating fully decomposed hydrazine and ammonia. Power was provided by a breadboard power processor. Performance was found to be a strong function of propellant flow rate. Anode losses were essentially constant for the range of mass flow rates tested. It is believed that the performance is dominated by viscous effects. Significantly improved performance was noted with simulated ammonia operation. At 300 W the specific impulse on simulated ammonia was 410 s with an efficiency of 0.34, while simulated hydrazine provided 370 s specific impulse at an efficiency of 0.27.

## INTRODUCTION

In the mid-1980's NASA and industry saw the need for advanced propulsion for large geosynchronous communication satellites (GEO comsats). At that time, state-of-art stationkeeping propulsion systems utilized chemical bipropellant thrusters or resistojets, which provided a specific impulse of approximately 300 s. Performance of those systems was limited by material temperature limits. By utilizing a different heating mechanism to raise the bulk gas temperature to levels exceeding materials limits, arcjets offered the potential of significantly increasing specific impulse and providing a correspondingly large on-board propellant savings.

The first NASA low-power arcjet development program was instituted in the 1980's and spurred the development of a commercial 1.8 kW hydrazine arcjet system

with a nominal mission average (NMA) specific impulse of 502 s.<sup>1</sup> That system is currently operational on the Telstar 401 spacecraft and baselined on 11 others. The second NASA arcjet program, the Arcjet Technology Development (ATD) Program, sought a step increase of 100 s specific impulse. To achieve that goal several technology insertions were necessary, including advanced refractory electrode materials and new low-erosion starting techniques. In a qualification representative test, the ATD program demonstrated over 1000 h of operation at a NMA specific impulse level exceeding 600 s.<sup>2</sup> With that successful demonstration, second generation, 600 s-class technology was transitioned to commercial production and is currently baselined for north-south stationkeeping on a new GEO comsat series. NASA's current arcjet program is targeted at providing advanced propulsion for power-limited satellites. Under the Low-Power Arcjet Thruster System (LPATS) program, a 0.5 kW hydrazine arcjet will be developed and demonstrated. The 0.5 kW

\*Aerospace Engineer, On-Board Propulsion Branch

\*\*Undergraduate, Mechanical Engineering Dept.

arcjet is of interest for both primary propulsion for near-Earth science missions and LEO comsat constellations and as auxiliary propulsion for power-limited GEO comsats.

All three of the aforementioned programs have had significant technology assessment portions completed in-house prior to the award of engineering model development contracts.<sup>3-5</sup> NASA's newest focus is on miniaturization of spacecraft to lower cost while maintaining mission goals. On-board propellant represents a major mass fraction of small spacecraft in many missions. The availability of high performance propulsion systems is mission enhancing and, in many cases, mission enabling.

To support NASA's smallsat program, research leading toward the development of a miniaturized arcjet system was initiated. The work is focused on determining whether arcjets can be scaled to operate reliably below 300 W at performance levels of interest to smallsats. Earlier research demonstrated throttleability from 100 W to 300 W with a subsonic-arc-attachment design; however, voltage instabilities were quite common and may increase the power processor complexity.<sup>6</sup> Preliminary research of supersonic-arc-attachment thrusters for the LPATS program demonstrated operation from 300 W to 800 W, but arc instabilities limited lower power operation.<sup>7</sup> A new thruster was designed to operate at nominally 300 W. This paper provides details of the new design and discusses measured performance and observed life issues.

## EXPERIMENTAL APPARATUS AND PROCEDURE

### Arcjet Thruster

A modular design philosophy was adopted to enable rapid replacement of parts. A cross-sectional schematic of the thruster is provided in Figure 1. The design was similar to previous 1 kW NASA Lewis

laboratory arcjets<sup>3</sup> with the following modifications. The anode formerly consisted of two pieces, a W/2 ThO<sub>2</sub> insert in a molybdenum housing. In the modified design, a single piece of W/2 ThO<sub>2</sub> was used. The rear-half of the thruster was brazed to insure hermetic integrity. Cathode/anode electrical isolation was provided by a commercial alumina isolator with tube ends. The ends were connected by modified fluid connectors and sealed using ferrules. Propellant injection was accomplished by radial grooves in the front insulator. Due to space limitations, the helical spring in the 1 kW design was replaced by Belleville washer springs which maintained compression as the parts expanded during operation.

The nozzle geometry was designed to promote supersonic-arc-attachment and is described in Table I. Both electrodes were machined from W/2 ThO<sub>2</sub>. The cathode was 1.6 mm in diameter with a 30° half-angle conical tip. The arc gap was set by withdrawing the cathode 0.25 mm from contact with the anode. The weight of the thruster was 0.18 kg.

### Power Supply

A breadboard power processing unit (PPU) designed to operate the arcjet in the 100-400 W range was used in this study and has been described in detail elsewhere.<sup>8</sup> The PPU operated with an input voltage range of 24-35 V and used a full bridge topology. The overall efficiency was 0.92. A high-voltage pulse of 3 kV provided by the PPU was used to ignite the thruster. Efforts are currently underway to develop a new breadboard power processor with flight-representative weight designed specifically for the miniature arcjet.

### Facility and Test Equipment

All testing was performed in an oil-diffusion pumped facility described previously.<sup>9</sup> The maximum facility pressure was 0.03 Pa ( $2 \times 10^{-4}$  torr) and was measured using ionization gages calibrated for air and uncorrected for sensitivity to

propellant gases. The thrust stand used is described elsewhere.<sup>10</sup> Thrust calibration was done *in-situ* by loading and unloading weights before, during, and after test runs. The uncertainty in the thrust measurement was determined to be  $\pm 0.5$  mN and attributable to thermal drift and hysteresis. All the efficiency values reported herein were calculated by dividing the thrust power by the input electrical power. Current was measured using a Hall-effect sensor with built-in calibration capability. Current signals were sent to a digital oscilloscope, and the voltage was measured using 100:1 probes.

Hydrogen and nitrogen at room temperature in ratios of 3:1 and 2:1 were used to simulate fully decomposed ammonia and hydrazine, respectively. The flow rate was regulated by thermal-conductivity-type flow controllers with a range of 0-2 SLPM and 0-5 SLPM for nitrogen and hydrogen, respectively. Calibration of the flow controllers was done *in-situ* by flowing the gas into an evacuated cylinder of known volume for a known time period. Using the initial and final pressures and temperatures of the gas and equation of state, the actual flow rate was determined. The uncertainty of the technique has been determined to be  $\pm 2\%$ .

## RESULTS AND DISCUSSION

### Electrical Characteristics

Figures 2a and 2b provide plots of the voltage/current (V/I) characteristics for both simulated ammonia and hydrazine, respectively, over a range of flow rates. In both cases the voltage was stable at all current levels tested (1.5 A to 2.5 A) for the highest flow rate (12 mg/s). Representative operation in this region is provided by the oscillogram shown in Figure 3. Voltage instabilities began to appear during operation at 10 mg/s at the lower limit of the current range. The instabilities consisted to two types. These were large random step changes in voltage of up to 30 V, noted during ammonia operation at 1.5 A, and high frequency

oscillations superimposed on the normal power supply ripple. The high frequency oscillations also occurred at random intervals and appeared at all points located below the region denoted as stable. With the exception of the 2A current level in the hydrazine test matrix, all operating points for both propellants at the lowest flow rate were unstable. The oscillogram provided in Figure 4 shows typical high frequency instabilities. The frequency of the oscillation was 1.6 MHz and had a sawtooth waveform with the voltage minimum of 115 V and a maximum of 125 V. The characteristics of the oscillations are very similar to those noted subsonic-arc-attachment thrusters. The "restrike" phenomenon documented in subsonic-arc-attachment thrusters is due to movement of the anode attachment point.<sup>11</sup>

### Performance

Performance data for the simulated ammonia and hydrazine propellants are shown in Tables II and III, respectively. Figures 5a and 5b provide plots of specific impulse and efficiency as functions of specific power for simulated ammonia and Figures 6a and 6b show similar data for hydrazine. The same basic trend was observed for operation on both propellants. As is typical with supersonic-arc-attachment thrusters, specific impulse steadily increased with specific power for all flow rates tested;<sup>5,7</sup> however, at a given specific power level, the specific impulse decreased rapidly with decreasing flow. The same effect is also illustrated in the plots of efficiency versus specific power provided in Figure 5b and 6b. Using the ammonia data at a specific power level of 30 MJ/kg as an example, the efficiency dropped from a high of 0.32 at 12.4 mg/s to 0.26 at 9.9 mg/s and finally to 0.18 at 7.4 mg/s. The reason for the effect is discussed further on in this section.

A comparison of performance between the two propellants is provided in Figure 7. For all three flow rates, both the efficiency and specific impulse were found to be higher for ammonia. Due to the lower

molecular weight of ammonia decomposition products when compared to hydrazine, it was expected that the specific impulse would be higher. What was unusual was the large difference in efficiency at a given flow rate. For example, at 300 W and at 12 mg/s the specific impulse was 410 s with an efficiency of 0.34 for ammonia, while hydrazine provided 370 s at 0.27.

An effort was made to determine the reason for the large effect of propellant hydrogen fraction and total flow rate on efficiency. Figure 8 details the energy deposition in an arcjet, and a more detailed description of arcjet thermal characteristics can be found elsewhere.<sup>12</sup>

Of the energy lost to the anode,  $Q_{\text{anode}}$ , some is recovered by regenerative heating of the incoming gas,  $Q_{\text{regen}}$ , and the remainder is radiated away,  $Q_{\text{rad}}$ .  $Q_{\text{regen}}$  is simply the mass flow rate times the enthalpy increase of the incoming gas. Hydrogen has a significantly larger heat capacity than nitrogen. With an increased hydrogen fraction, cold incoming simulated ammonia should absorb more heat. An estimate of the amount of heat absorbed by the incoming gas was made using hydrogen and nitrogen thermodynamic properties and assuming both that the nozzle was isothermal and that the incoming gas reached the nozzle temperature. The results, provided in Table IV, indicate that the fraction of energy recovered regeneratively is not a strong function of propellant mixture or of flow rate.

Since the effects are not accounted for by a regenerative effect, the next logical assumption is that the anode losses were both greater for hydrazine than ammonia and increase with decreasing flow rate. The following shows that not to be true. Estimates made for  $Q_{\text{rad}}$  combined with  $Q_{\text{regen}}$  allowed  $Q_{\text{anode}}$  to be determined. The results presented in Table IV show that at a given specific power level, the anode losses were essentially independent of flow rate and were estimated to be approximately 0.19 to 0.23 of the input

power. Interestingly, a similar fraction was found to be lost in a larger 1 kW thruster.<sup>12</sup> In light of the above results, the cause for the efficiency difference between ammonia and hydrazine is unclear; however, it is suspected that the decrease in efficiency with flow rate may be due to increased viscous losses in the nozzle. If viscous effects are a major loss, optimizing the geometry may provide improved performance.

The testing sequence was such that the ammonia data were obtained, followed by the hydrazine, and then the ammonia data were repeated. Data were taken over the course of several days, and the final performance data matched the initial. Also, the mass flow rate for each test run was held constant, and data were obtained at constant current levels in random order.

#### Life Issues

Endurance testing of the thruster was beyond the scope of this study; however, anode erosion issues with the current design appear life limiting. Post test examination of the nozzle showed severe erosion in the constrictor. Photomicrographs of both ends of the constrictor are provided in Figure 9. Material was removed from the converging section and deposited downstream, probably during start-up. Radial cracking was also noted, and the throat had an irregular shape. Advanced tungsten alloys such as W/4Re/0.35HfC could increase the yield strength and possibly prevent some of the deformation. That material was not used in this study due to fabrication issues, availability, and cost.

Life issues concerning the cathode were also identified. On several occasions following shutdown, the thruster could not be restarted and was found to be electrically shorted. Deformation of the cathode is noted in the post-test photomicrograph shown in Figure 10. The original cathode had a sharp tip machined, and after operation the tip had receded with a small molten nodule remaining. Molten cathode material was found to bulge out near the tip and is suspected to be the cause of the

short. Also, approximately 1 mm upstream of the shoulder, molten spots were noted along the circumference of the cathode. Propellant was injected radially toward the cathode and stagnated at that point. It is thought that at arc ignition, the higher local pressure caused arc attachment in that area. Design changes need to be implemented to reduce the effects of cathode deformation to increase long-life reliability.

### CONCLUDING REMARKS

A laboratory model miniaturized arcjet was designed and tested at power levels from 200-400 W and had a mass of 0.18 kg. Operating characteristics were obtained on nitrogen/hydrogen mixtures simulating fully decomposed ammonia and hydrazine. Voltage instabilities increased with a decrease in flow rate and consisted mainly of high frequency oscillations; however, large step changes in voltage were also noted at some operating points below 300 W.

Ammonia performance was substantially higher than hydrazine. At the nominal power level of 300 W, ammonia produced a specific impulse of 410 s with an efficiency of 0.34 while similar operation on hydrazine provided 370 s specific impulse at an efficiency of 0.27. The reason for the large difference is not currently understood. For both propellants at a given specific power level the performance degraded dramatically with decreased flow rate. For example, the efficiency for ammonia at a specific power level of 30 MJ/kg dropped from 0.32 at 12.4 mg/s to 0.18 at 7.4 mg/s. The fraction of energy lost to the anode and the fraction of energy recovered regeneratively were determined to be relatively constant with flow rate. It is believed that viscous losses in the nozzle increase significantly with the decreased flow rates, causing the loss in performance.

Although performance was repeatable at the beginning and end of the study, post-test examination of the electrodes showed erosion to be severe and probably life-

limiting. Erosion of the anode may be decreased through the use of advanced refractory alloys and improved starting techniques. Cathode deformation caused shorting of the thruster and needs to be further addressed.

Steady operation at 300 W has been successfully demonstrated at performance levels significantly improved over chemical and resistojet systems. Development efforts must now focus on systems issues including mass reduction and long-life operation.

### REFERENCES

1. Smith, R.D., *et al.*, "Flight Qualification of a 1.8 kW Hydrazine Arcjet System," *Proceedings of the 23rd International Electric Propulsion Conference*, Sept. 1993, pp. 93-107.
2. McLean, C.H., Lichon, P.G., and Sankovic, J.M., "Life Demonstration of a 600-Second Mission Average Arcjet," AIAA-Paper-94-2866, June 1994.
3. Curran, F.M. and Haag, T.W., "Extended Life and Performance Test of a Low-Power Arcjet," *J. of Spacecraft and Rockets*, Vol. 29, No. 4, July-Aug. 1992, pp. 444-452.
4. Gruber, R.P., "Power Electronics for a 1-Kilowatt Arcjet Thruster," AIAA-Paper-86-1507 (also NASA TM 87340), June 1986.
5. Curran, F.M. and Sarmiento, C.J., "Low Power Arcjet Performance," AIAA-Paper-90-2578 (also NASA TM 103280), July 1990.
6. Sankovic, J.M., "Ultra-Low-Power Arcjet Thruster Performance," *Proceedings of the 1993 JANNAF Propulsion Meeting*, Vol. V, CPIA, Nov. 1993, pp. 371-386.

7. Pencil, E.J., *et al.*, "Subkilowatt Arcjet Development," *Proceedings of the 24th International Electric Propulsion Conference*, Sept. 1995. *to be published.*
8. Hamley, J.A. and Hill, G.M., "Power Electronics for Low Power Arcjets," AIAA-Paper-91-1991 (also NASA TM 104459), June 1991.
9. Sankovic, J.M. and Berns, D.H., "Performance of a Low-Power Subsonic-Arc-Attachment Arcjet Thruster," AIAA-Paper-93-1898 (also NASA TM 106244), June 1993.
10. Haag, T.W. and Curran, F.M., "Arcjet Starting Reliability: A Multistart Test," AIAA-87-1060 (also NASA TM 89857), May 1987.
11. Berns, D.H., and Sankovic, J.M., "Investigation of a Subsonic-Arc-Attachment Thruster Using Segmented Anodes," AIAA-Paper-93-1899, June 1993.
12. Sankovic, J.M. and Curran, F.M., "Arcjet Thermal Characteristics," AIAA-Paper-91-2456 (also NASA TM 105156), June 1991.

Table I. Nozzle parameters

Constrictor Diameter (mm)	0.25
Constrictor Length (mm)	0.13
Nozzle Area Ratio	400
Nozzle Divergent Half-Angle	15°
Nozzle Convergent Half-Angle	30°

Table II. Simulated ammonia performance

Current	Voltage	Power	Thrust	Mass flow	Specific Impulse	Efficiency	Specific Power
A	V	W	mN	mg/s	s		MJ/kg
1.50	182	273	48.7	12.4	399	0.349	21.9
1.75	170	298	49.9	12.4	409	0.337	23.9
2.00	165	331	51.8	12.4	424	0.325	26.6
2.25	162	365	53.7	12.4	439	0.317	29.3
2.50	156	391	55.4	12.4	454	0.315	31.4
2.00	165	329	52.3	12.4	428	0.333	26.4
1.50	140	210	36.9	9.9	378	0.326	21.1
2.00	156	313	39.9	9.9	410	0.256	31.5
2.25	152	342	41.4	9.9	424	0.252	34.4
2.50	146	364	42.7	9.9	438	0.252	36.7
1.75	164	288	39.8	9.9	409	0.278	29.0
1.50	167	250	38.2	9.9	391	0.292	25.2
2.00	158	316	41.5	9.9	426	0.275	31.8
1.50	133	200	22.2	7.4	305	0.167	26.9
1.75	125	219	24.5	7.4	338	0.186	29.5
2.00	127	254	25.3	7.4	348	0.170	34.3
2.25	128	287	26.4	7.4	363	0.164	38.7
2.00	147	294	26.8	7.4	368	0.164	39.7



Table III. Simulated hydrazine performance

Current	Voltage	Power	Thrust	Mass flow	Specific Impulse	Efficiency	Specific Power
A	V	W	mN	mg/s	s		MJ/kg
1.50	160	240	41.3	12.3	341	0.288	19.5
2.00	154	308	45.1	12.3	372	0.267	25.0
2.25	148	334	46.5	12.3	384	0.263	27.0
2.50	144	359	47.8	12.3	394	0.257	29.1
1.75	161	282	44.6	12.3	368	0.286	22.8
2.00	155	310	45.7	12.3	378	0.274	25.1
1.50	131	197	28.5	9.8	296	0.211	20.0
2.00	143	286	34.0	9.8	353	0.207	29.1
2.25	139	312	35.9	9.8	373	0.210	31.8
2.50	135	338	37.1	9.8	385	0.208	34.4
1.75	147	257	33.6	9.8	349	0.224	26.2
2.00	140	280	34.5	9.8	358	0.216	28.5
1.50	122	182	18.6	7.3	256	0.129	24.6
2.00	135	270	22.8	7.3	313	0.130	36.5
1.75	129	226	21.7	7.3	298	0.141	30.5
2.00	130	260	22.8	7.3	313	0.135	35.1

Table IV. Energy deposition estimates

H2:N2 Ratio	Current	Power	Specific Power	Mass flow	Anode Temperature	Qrad	Qregen	Qanode	Qanode/Power	Qregen/Power
	A	W	MJ/kg	mg/s	°C	W	W	W		
2:1	2.50	359	29.1	12.3	1194	34	49	83	0.23	0.14
2:1	2.00	286	29.1	9.8	1140	30	37	67	0.23	0.13
2:1	1.75	226	30.5	7.3	1095	26	27	53	0.23	0.12
3:1	2.25	365	29.3	12.4	1082	25	45	70	0.19	0.12
3:1	1.75	288	29.0	9.9	1047	22	35	57	0.20	0.12
3:1	1.75	219	29.5	7.4	1078	25	27	51	0.23	0.12

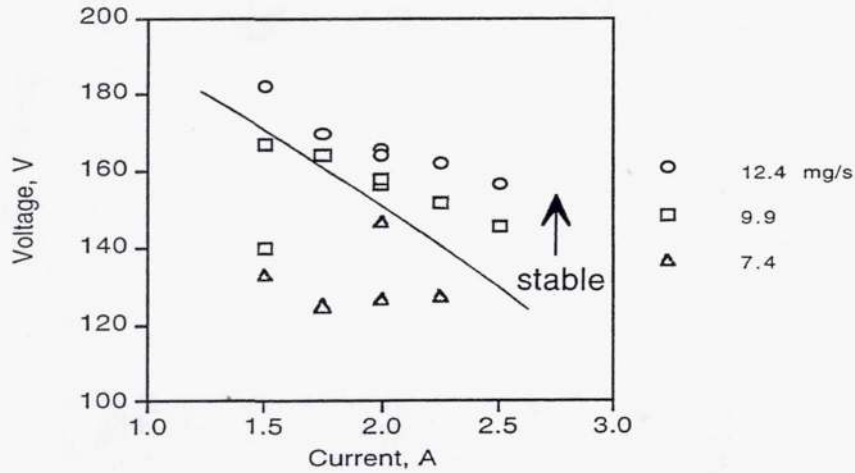
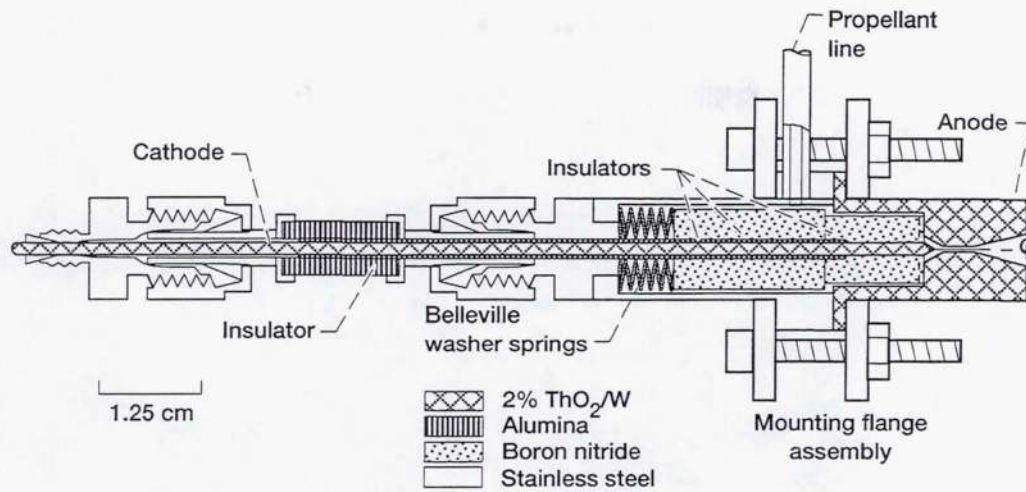


Figure 2a. Simulated ammonia

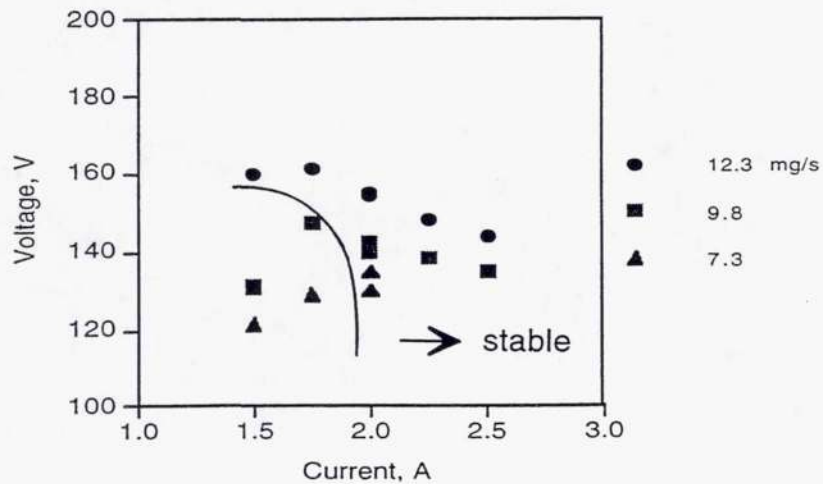


Figure 2b. Simulated hydrazine

Figure 2. Electrical characteristics

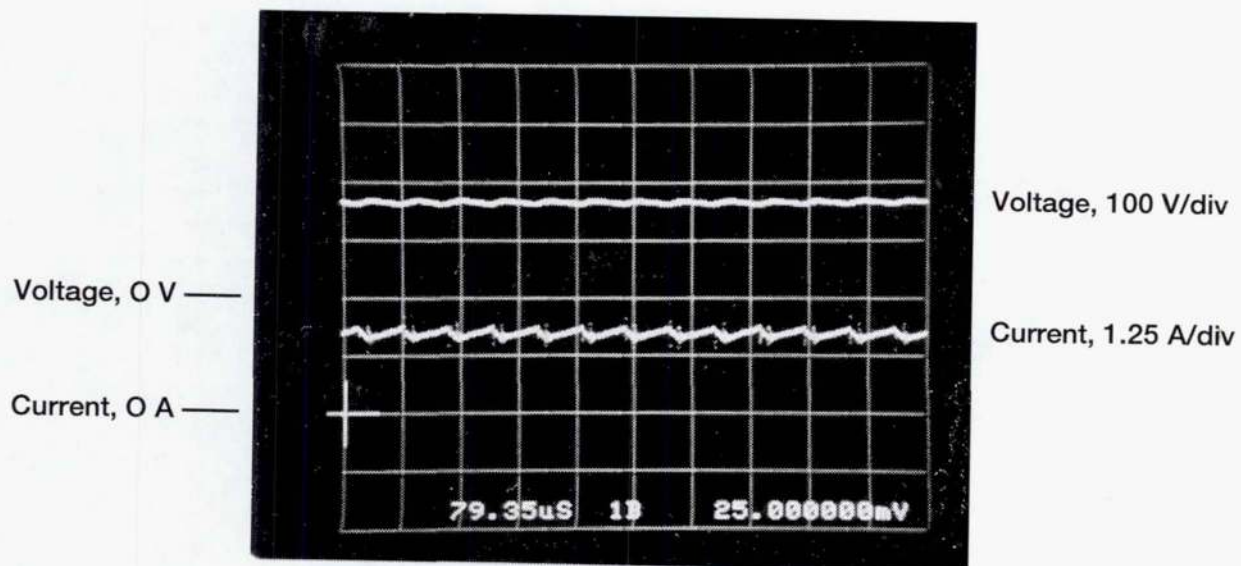


Figure 3. Typical oscillogram of stable operation. Simulated ammonia; 12.4 mg/s; 2 A; 165 V. Time scale 79.35 microseconds/div.

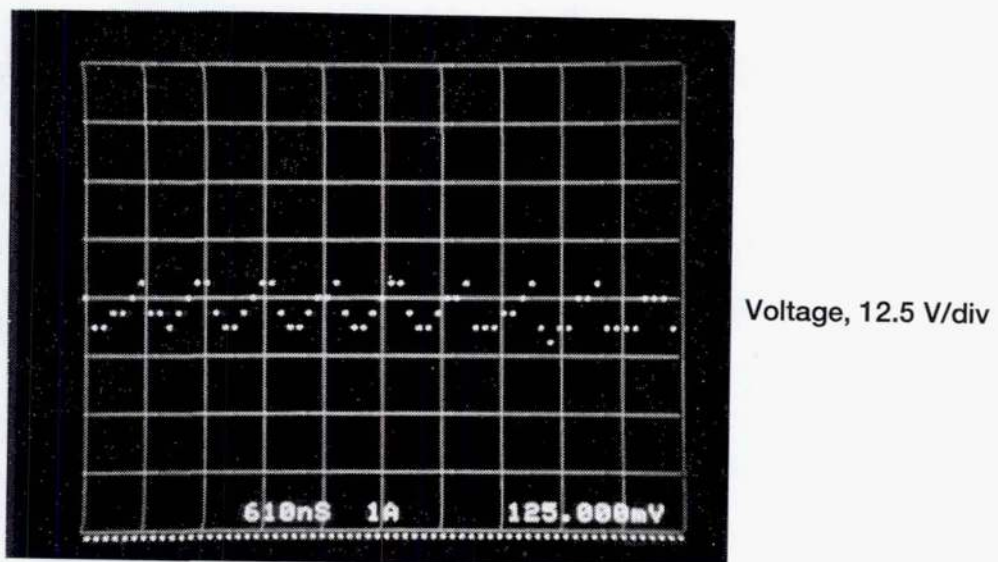


Figure 4. Typical oscillogram of high frequency instability. Simulated hydrazine; 7.3 mg/s; 1.5 A; 122 V. Time scale 610 nanoseconds/div.

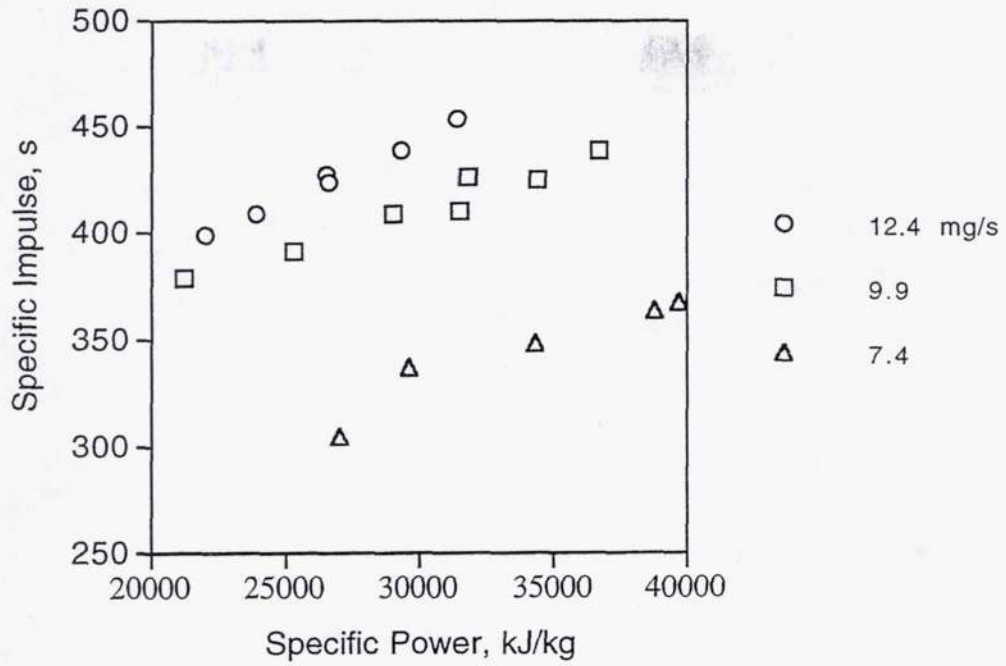


Figure 5a. Specific impulse versus specific power

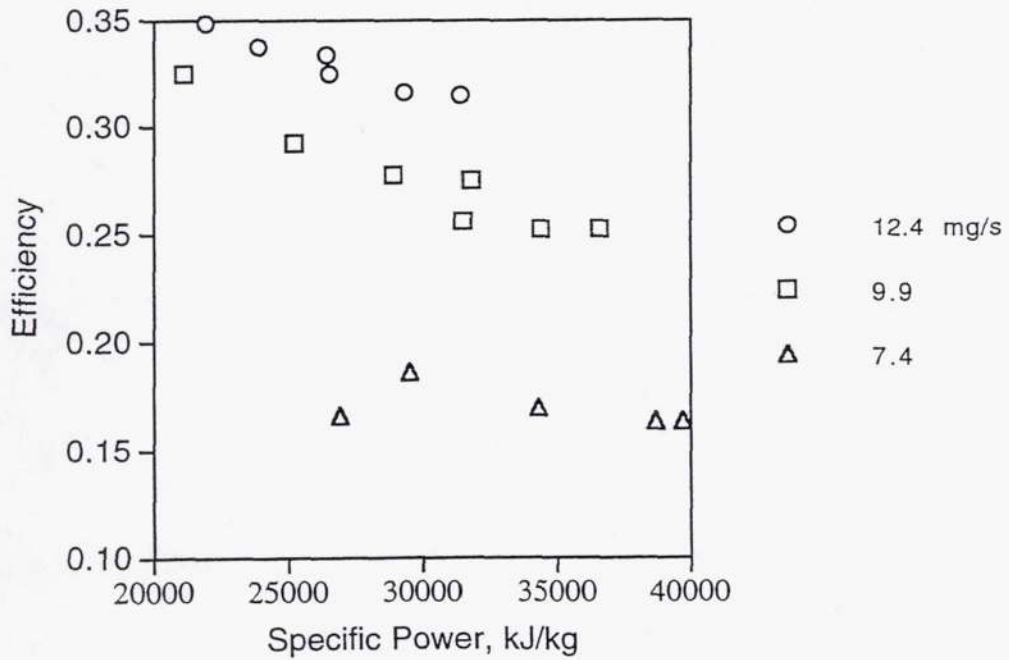


Figure 5b. Efficiency versus specific power

Figure 5. Simulated ammonia performance

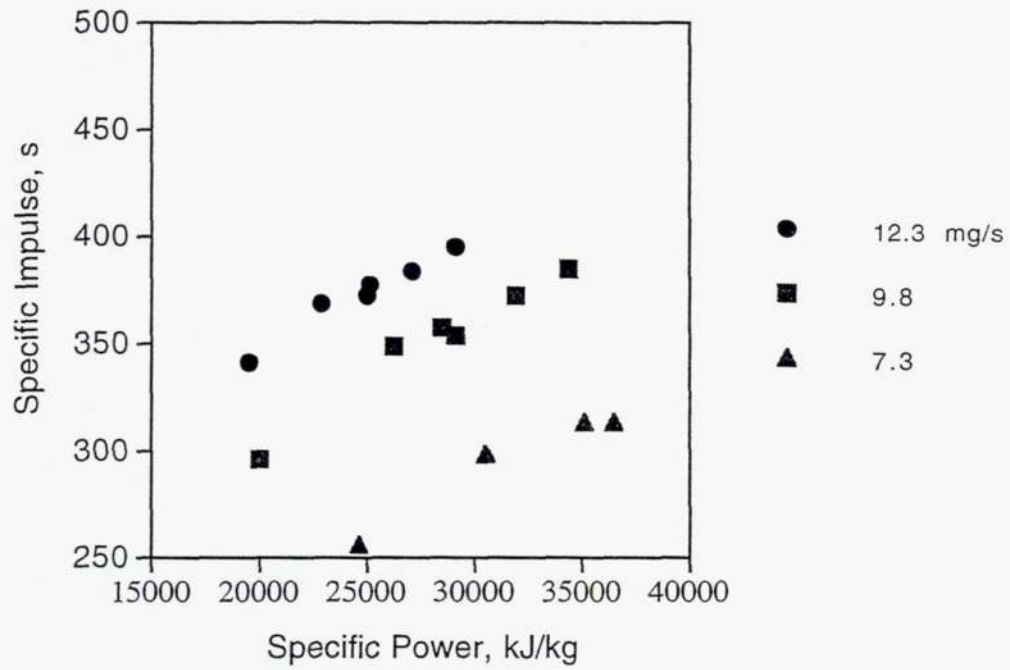


Figure 6a. Specific impulse versus specific power

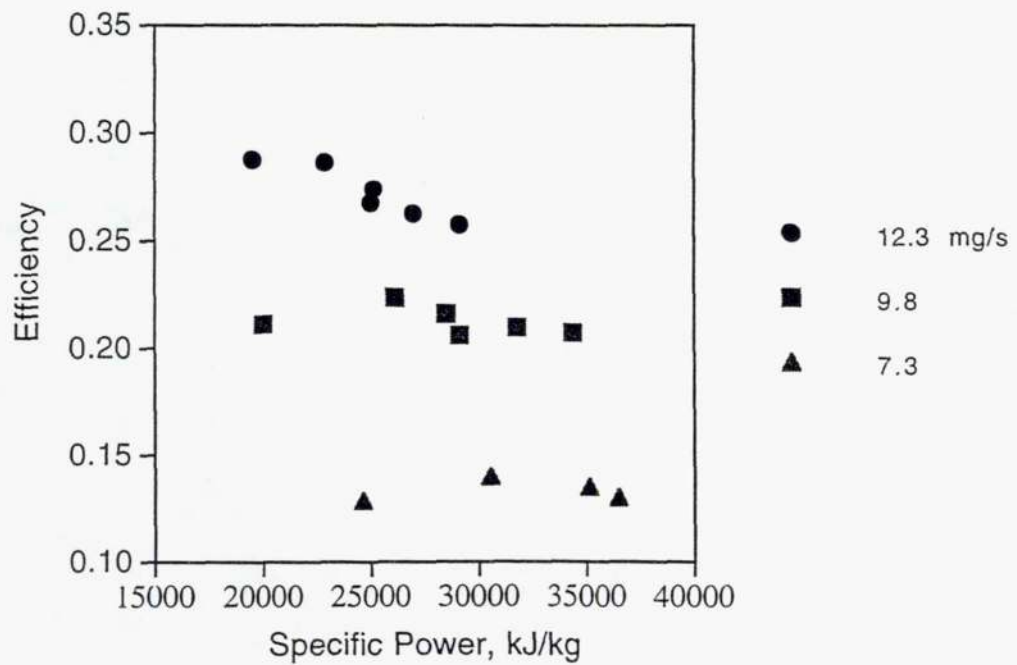


Figure 6b. Efficiency versus specific power

Figure 6. Simulated hydrazine performance

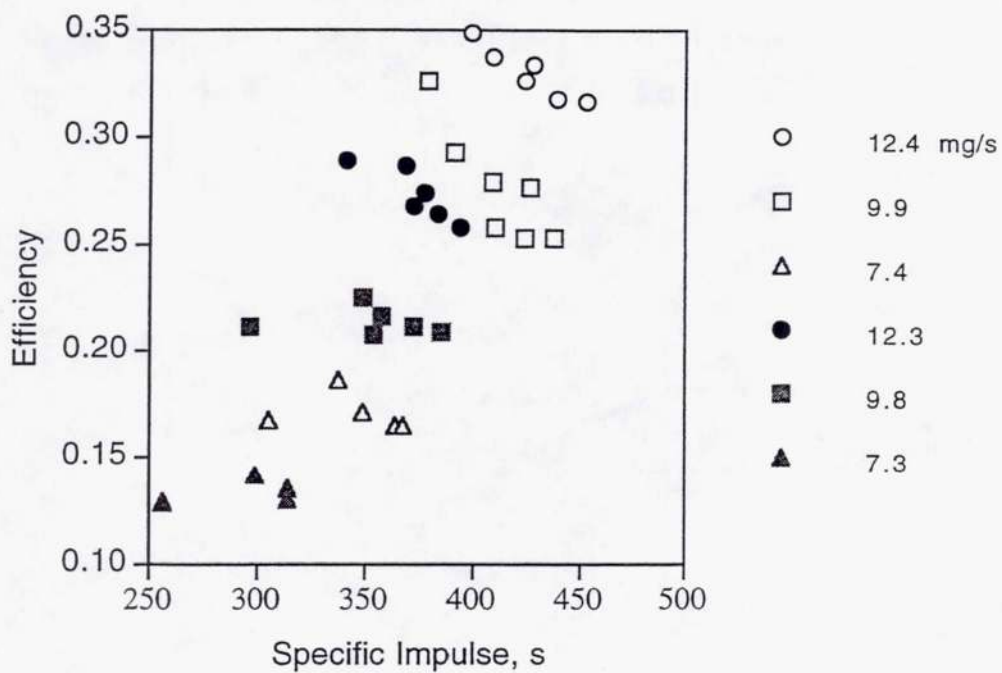


Figure 7. Efficiency versus specific impulse. 3:1 H<sub>2</sub>:N<sub>2</sub> open symbols; 2:1 H<sub>2</sub>:N<sub>2</sub> closed symbols

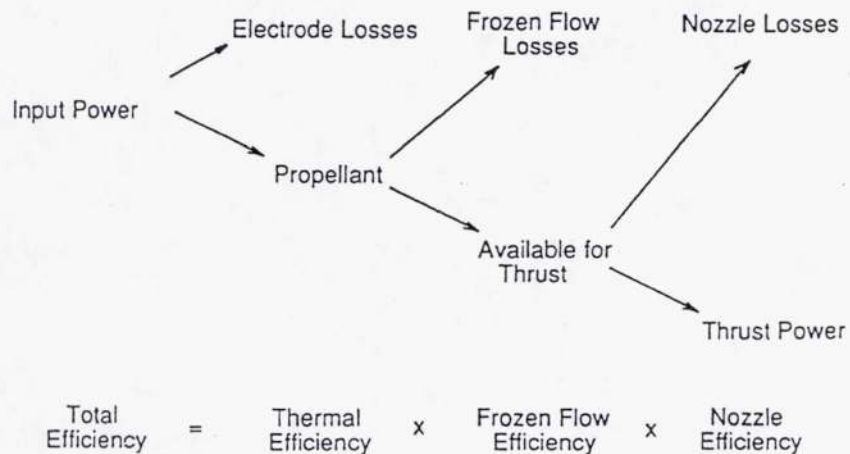


Figure 8. Energy deposition in an arcjet. (from Reference12)



Figure 9a. Converging side.



Figure 9b. Diverging side.

Figure 9. Post-test scanning electron micrograph of anode.

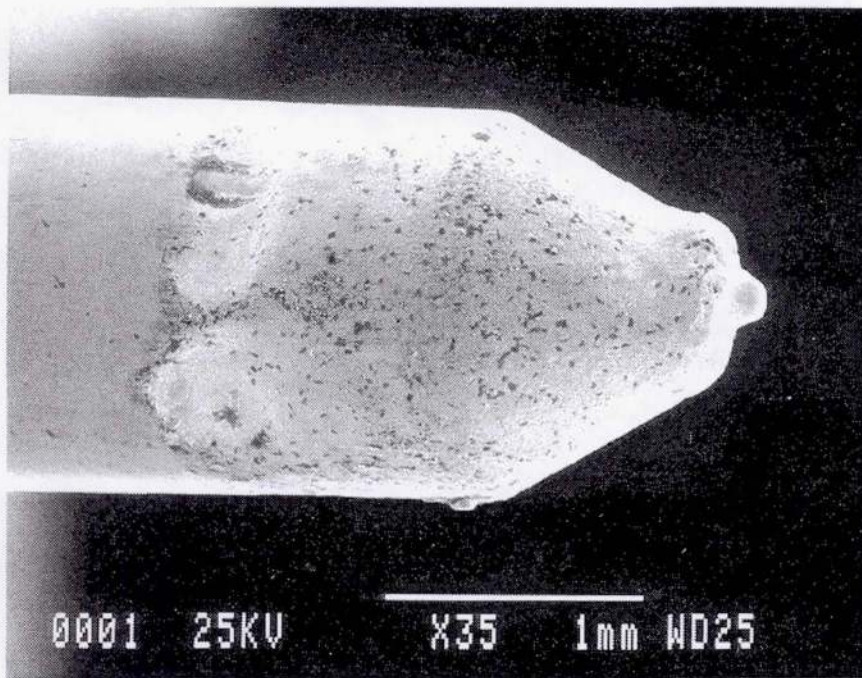


Figure 10. Post-test scanning electron micrograph of cathode.



# REPORT DOCUMENTATION PAGE

Form Approved  
OMB No. 0704-0188

Public reporting burden for this collection of information is estimated to average 1 hour per response, including the time for reviewing instructions, searching existing data sources, gathering and maintaining the data needed, and completing and reviewing the collection of information. Send comments regarding this burden estimate or any other aspect of this collection of information, including suggestions for reducing this burden, to Washington Headquarters Services, Directorate for Information Operations and Reports, 1215 Jefferson Davis Highway, Suite 1204, Arlington, VA 22202-4302, and to the Office of Management and Budget, Paperwork Reduction Project (0704-0188), Washington, DC 20503.

1. AGENCY USE ONLY (Leave blank)	2. REPORT DATE November 1995	3. REPORT TYPE AND DATES COVERED Technical Memorandum	
4. TITLE AND SUBTITLE  Performance of a Miniaturized Arcjet		5. FUNDING NUMBERS  WU-242-70-02	
6. AUTHOR(S)  John M. Sankovic and David T. Jacobson		8. PERFORMING ORGANIZATION REPORT NUMBER  E-9923	
7. PERFORMING ORGANIZATION NAME(S) AND ADDRESS(ES)  National Aeronautics and Space Administration Lewis Research Center Cleveland, Ohio 44135-3191		10. SPONSORING/MONITORING AGENCY REPORT NUMBER  NASA TM-107062 AIAA-95-2822	
9. SPONSORING/MONITORING AGENCY NAME(S) AND ADDRESS(ES)  National Aeronautics and Space Administration Washington, D.C. 20546-0001		11. SUPPLEMENTARY NOTES Prepared for the 31st Joint Propulsion Conference and Exhibit cosponsored by AIAA, ASME, SAE, and ASEE, San Diego, California, July 10-12, 1995. John M. Sankovic, NASA Lewis Research Center and David T. Jacobson, The Ohio State University, Columbus, Ohio 43210. Responsible person, John M. Sankovic, organization code 5330, (216) 977-7429.	
12a. DISTRIBUTION/AVAILABILITY STATEMENT  Unclassified - Unlimited Subject Category 20  This publication is available from the NASA Center for Aerospace Information, (301) 621-0390.		12b. DISTRIBUTION CODE	
13. ABSTRACT (Maximum 200 words)  Performance measurements were obtained and life-limiting mechanisms were identified on a laboratory-model arcjet thruster designed to operate at a nominal power level of 300 W. The design employed a supersonic-arc-attachment concept and was operated from 200 to 400 W on hydrogen/nitrogen mixtures in ratios simulating fully decomposed hydrazine and ammonia. Power was provided by a breadboard power processor. Performance was found to be a strong function of propellant flow rate. Anode losses were essentially constant for the range of mass flow rates tested. It is believed that the performance is dominated by viscous effects. Significantly improved performance was noted with simulated ammonia operation. At 300 W the specific impulse on simulated ammonia was 410 s with an efficiency of 0.34, while simulated hydrazine provided 370 s specific impulse at an efficiency of 0.27.			
14. SUBJECT TERMS  Arcjet thruster; Electric propulsion; Satellite propulsion		15. NUMBER OF PAGES 17	
		16. PRICE CODE A03	
17. SECURITY CLASSIFICATION OF REPORT Unclassified	18. SECURITY CLASSIFICATION OF THIS PAGE Unclassified	19. SECURITY CLASSIFICATION OF ABSTRACT Unclassified	20. LIMITATION OF ABSTRACT